Fine structure of exciton complexes in high-symmetry quantum dots: Effects of symmetry breaking and symmetry elevation

K. F. Karlsson,[1,2] M. A. Dupertuis,[1] D. Y. Oberli,[1] E. Pelucchi,[1] A. Rudra,[1] P. O. Holtz,[2] and E. Kapon[1]

[1]*Ecole Polytechnique Fédérale de Lausanne (EPFL), Laboratory of Physics of Nanostructures, CH-1015 Lausanne, Switzerland*
[2]*Department of Physics, Chemistry, and Biology (IFM), Semiconductor Materials, Linköping University, S-58183 Linköping, Sweden*

Quantum dots (QDs) of high symmetry (e.g., C_{3v}) have degenerate bright exciton states, unlike QDs of C_{2v} symmetry, making them intrinsically suitable for the generation of entangled photon pairs. Deviations from C_{3v} symmetry are detected in real QDs by polarization-resolved photoluminescence spectroscopy in side-view geometry of InGaAs/AlGaAs dots formed in tetrahedral pyramids. The theoretical analysis reveals both an additional symmetry plane and weak symmetry breaking, as well as the interplay with electron-hole and hole-hole exchange interactions manifested by the excitonic fine structure.

Semiconductor quantum dots (QDs) exhibit atomiclike energy spectra potentially useful in the area of quantum-information processing. The indistinguishable radiation paths of the biexciton cascade decay have been proposed as the source of polarization-entangled photons.[1] In the conventional QD fabrication process the nucleation of strained InAs QDs occurs spontaneously on the (001) plane of Zincblende crystals. The symmetry of these QDs is thus limited by the crystal to C_{2v}.[2] The resulting anisotropy of the confined exciton breaks the degeneracy of its bright states, which prohibits entanglement and produces a fine structure splitting (FSS) characterized by the emission of two linearly polarized photons of unequal energies. Nevertheless, entangled photon pairs from such QDs have been detected by means of careful preselection of particular QDs,[3,4] by spectral postselection,[5] at the price of losing photons, or by the heavy use of external magnetic fields to restore the intermediate level degeneracy.[6] In the quest of more efficient QD sources of entangled photons, it was recently predicted that replacing the conventional GaAs barriers by InP significantly reduces the exciton FSS in such InAs self-assembled QDs.[7] Until now, however, studies of the FSS of neutral and charged exciton complexes have been limited to QDs of C_{2v} or lower symmetry.[2–11]

In this Rapid Communication, we experimentally and theoretically investigate the FSS in QDs with high symmetry. Zincblende QDs of C_{3v} symmetry can ideally be achieved by choosing [111] as the crystallographic direction of crystal growth instead of the conventional [001] direction. For this growth geometry, including the lack of inversion symmetry in the crystal and the effects of strain and piezoelectric fields, the minimal symmetry is C_{3v} as long as the QD heterostructure has symmetrical shape. Here we utilize InGaAs/AlGaAs QDs that allow the simultaneous study of the FSS of dominating heavy-hole (hh) and light-hole (lh) excitons as well as a hybrid hh-lh trion by side-view polarization-resolved photoluminescence (PL) spectroscopy. We show how these trion states can probe a small symmetry breaking in otherwise ideal C_{3v} QDs due to exchange interactions.

The polarization properties of the exciton fine structure depend on the symmetries of the initial and final states with respect to the electric dipole. Given the symmetries of every electron and hole state, the optical selection rules and corresponding decay schemes are obtained by the Wigner-Eckart theorem for point groups. However, numerical computations involving band mixing and many-body effects are required to quantitatively determine the energies and the intensities of the optical transitions.

Figure 1 presents several dot structures with various degrees of symmetry and the related excitonic transitions of interest here. The symmetry of the C_{3v} electron ground state is restricted to $E_{1/2}$ while hole symmetries can be $E_{3/2}$ or $E_{1/2}$ using the double group notation of Ref. 12. Thus, two types of excitons can be formed due to the two possible hole symmetries. The radiative decay of type one, a C_{3v} exciton formed with a $E_{3/2}$ hole, is schematically shown in Fig. 1(b) (left), where the order of the energy levels is chosen consistent with both experimental data and numerical calculations. Group theory predicts that this exciton exhibits two pairs of degenerate bright states, decaying with pure and isotropic in-plane (xy) polarization. The corresponding transitions related to the elevated symmetry D_{3h}, with horizontal symmetry plane [see Fig. 1(a)], are indicated in the same figure [Fig. 1(b) (left)], where only the thick lines are optically active in D_{3h} symmetry. Hence, a D_{3h} exciton has dark states. For the second type of exciton, formed by an electron and an $E_{1/2}$ hole, the decay scheme is identical for C_{3v} and D_{3h}, as shown
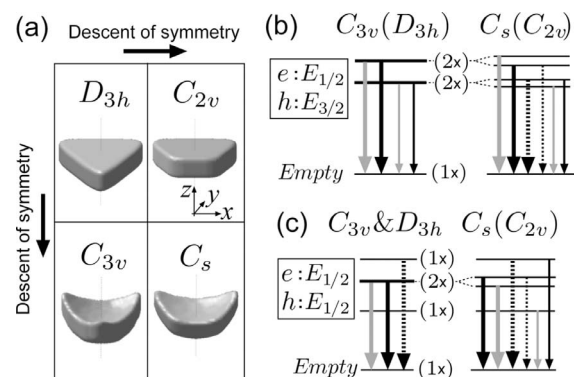
FIG. 1. (a) Symmetry hierarchy visualized by three-dimensional objects. (b) and (c) Polarized radiative decay paths of C_{3v} excitons formed with holes of $E_{3/2}$ and $E_{1/2}$ symmetries, and the corresponding decay of C_s excitons. Transitions allowed for $C_{3v}(C_s)$ but forbidden under $D_{3h}(C_{2v})$ are distinguished by thin lines and small arrows. Gray (black) lines indicate x-polarized (y-polarized) light. Dotted lines indicate z-polarized light.
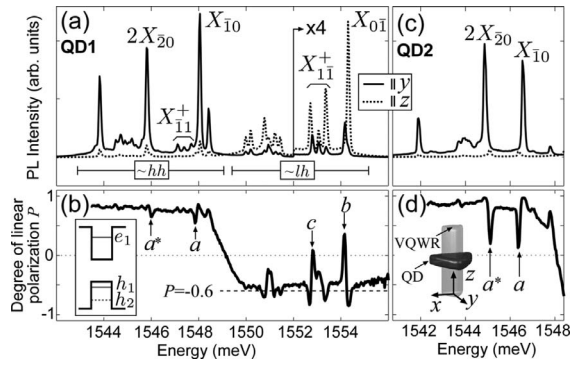
FIG. 2. (a) and (c) Polarized PL spectra of two QDs and (b) and (d) the corresponding degree of linear polarization. The PL is recorded for polarization vectors perpendicular (solid lines) and parallel (dotted lines) to the growth direction z. The insets illustrate schematic diagrams of (b) single particle energy levels and (d) the QD geometry.

in Fig. 1(c) (left): one state is bright with a vertical polarization vector (z), two other states are bright with isotropic in-plane polarization and one state is dark. Hence, C_{3v} and D_{3h} excitons exhibit the in-plane polarized degenerate bright states required for photon entanglement.[13]

A perturbation of the QD shape that reduces the symmetry from $C_{3v}(D_{3h})$ to $C_s(C_{2v})$ [see Fig. 1(a)], likely to occur in real structures, induces optical anisotropy. The corresponding decay schemes are obtained by subduction and shown on the right in Figs. 1(b) and 1(c). In all cases the degenerate bright states split by the anisotropic part of the electron-hole exchange interaction. Moreover, the C_{3v} and D_{3h} excitons of type one ($E_{3/2}$ hole), which decay with pure in-plane polarization, yield vertically polarized components after perturbation [Fig. 1(b) (right)].

The experimental investigations are performed on arrays of uniform QDs fabricated by low-pressure organometallic chemical vapor deposition in inverted tetrahedral micropyramids patterned on a 2°-off GaAs (111)B substrate.[14] Thin QDs ($\sim$1.5 nm) are self-formed due to growth anisotropy and capillarity effects[15] from a nominally 0.5-nm-thick $In_{0.10}Ga_{0.90}As$ layer at the center of the pyramids, sandwiched between $Al_{0.30}Ga_{0.70}As$ barriers. The actual Al concentration in the barriers surrounding the QD is however lower due to alloy segregation, as a vertical quantum wire (VQWR) of nearly pure GaAs ($\sim$4% Al content) is formed at the center of the pyramid intersecting the QD.[16] The inset of Fig. 2(d) illustrates a simplified QD geometry and defines the vertical growth direction z [111], and the in-plane directions x [1$\bar{1}$0] and y [11$\bar{2}$] (see Ref. 17 for a detailed description of the geometry). Individual QDs were excited by a laser (wavelength 532 nm, power $\sim$50 nW) and studied at low temperatures ($<$30 K) by means of a micro-PL setup ($\sim$1 μm spot size) with a spectral resolution of 110 μeV.[14] The sample was cleaved along the y direction and the PL was collected from the cleaved edge along the x direction. The linear polarization content in the yz plane was analyzed (contrast: 50:1) by rotation of a $\lambda/2$ phase retardation plate preceding a fixed linear polarizer in the signal path. More than 15 QDs where studied, represented by spectra of two QDs (QD1–2) discussed here.

All the emission lines present in typical PL spectra, as the ones shown in Fig. 2(a), have been rigorously identified experimentally by controlled charge tuning, temporal photon correlation and polarization measurements.[18–20] Two groups of emission lines are distinguished by the sign of linear polarization $P = (I_y - I_z)/(I_y + I_z)$, where $I_{y(z)}$ is the PL intensity linearly polarized along y or z [Fig. 2(b)]. In a previous study we related P to the polarization selection rules of hh ($I_z:I_y = 0:3 \Rightarrow P = 1$) and lh ($I_z:I_y = 4:1 \Rightarrow P = -0.6$) valence band states and concluded that the first hole level (h_1) is hh-like and the second level (h_2) is lh-like [inset of Fig. 2(b)].[18]

An *exciton* is labeled $X_{n_1 n_2}$, where $n_i = \{0, 1, 2\}$ denotes the occupancy of holes in single particle level h_i. Biexcitons are prefixed with 2 and positive trions have the superscript +. In this Rapid Communication, the attention is restricted to the hh-like exciton (X_{10}) and biexciton ($2X_{20}$), to the lh-like exciton (X_{01}) and to the hh-lh hybrid trion (X_{11}^+). Optical *transitions* involving the hole in level i are marked by a bar above n_i (e.g., $X_{1\bar{1}}^+$).[21]

Some exciton lines exhibit strong deviation from the local average value of P as indicated by arrows (a, a^*, b, and c) in Figs. 2(b) and 2(d). For example, a distinct dip a is systematically observed on the low-energy side of $X_{\bar{1}0}$ always accompanied by a dip a^* on the high-energy side of $2X_{\bar{2}0}$. The coexistence of a and a^* suggests an association with the exciton fine structure; upon decay of the closed-shell biexciton the spectral features of $2X_{\bar{2}0}$ are simply the mirrored ones of $X_{\bar{1}0}$. At closer inspection, a weak z-polarized component is resolved $\sim$200 μeV below the y-polarized main peak of $X_{\bar{1}0}(I_z:I_y = 0.2:3)$, as shown in Fig. 3(a). Also $X_{0\bar{1}}$ exhibits two components ($I_z:I_y = 4:0.97$) but the energy order is reversed, as compared to $X_{\bar{1}0}$, and the energy separation is smaller, $\sim$140 μeV [Fig. 3(b)]. The trion signature is more complicated and it will be discussed in the last part of this Rapid Communication.

The agreement between the experimental data, group theoretical arguments and numerical calculations suggests that X_{01} is formed with an $E_{1/2}$ hole: two spectral components, linearly polarized in-plane and vertically, are resolved for $X_{0\bar{1}}$ [Figs. 3(b) and 1(c) (left)]. On the other hand, $X_{\bar{1}0}$ mainly exhibits in-plane polarization [Fig. 3(a)], reminding about the pure in-plane polarization of an exciton with an $E_{3/2}$ hole [Fig. 1(b) (left)]. However, a weak vertically polarized component is resolved for $X_{\bar{1}0}$, indicating either that the hole actually possesses $E_{1/2}$ symmetry [Fig. 1(c) (left)] or that the QD is slightly asymmetric [Fig. 1(b) (right)].

In order to determine the hole symmetries and quantitatively estimate the exciton fine structure by theoretical means, the QD system is modeled within the 8×8 band envelope function approximation ($k \cdot p$).[22] The chosen geometry is an 1.5-nm-thick flat $In_{0.10}Ga_{0.90}As$ QD of triangular cross section [inset of Fig. 3(c), $a = 16$ nm] surrounded by $Al_{0.20}Ga_{0.80}As$ since Al-Ga segregation reduces the Al concentration from its nominal value of 30%.[16] Furthermore, a finite GaAs VQWR (length: 26 nm) of identical cross section as the QD intersects the dot symmetrically along z. The inherent strain due to the lattice mismatch is simulated by continuum elastic theory. The assumed QD shape has D_{3h} symmetry but the confined states anyway display only C_{3v}
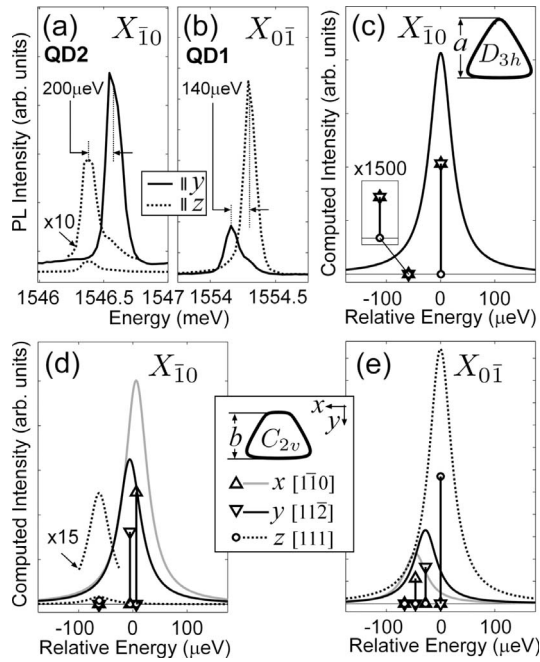
FIG. 3. Close-up PL of (a) $X_{\bar{1}0}$ and (b) $X_{0\bar{1}}$. Computed exciton spectra for (c) a symmetric QD, (d)–(e) an asymmetric QD. A Lorentzian broadening parameter (50 μeV) is introduced in (c)–(e). Unbroadened stems are also shown. The insets define polarization directions, and the shape and orientation of the computed QD ($a=16$ nm, $b=12.5$ nm).

symmetry due to both the strain-induced piezoelectric field and the bulk $k \cdot p$ Hamiltonian. For this model, one single electron level (e_1) and three hole levels (h_{1-3}) are confined in the QD. e_1, h_1, and h_2 have dominating s-like envelope wave functions exhibiting $E_{1/2}$, $E_{3/2}$, and $E_{1/2}$ symmetries, respectively. The hole character, with respect to z, for h_1 is 89% hh and for h_2 it is 91% lh, i.e., nearly pure hh and lh characters in accordance with earlier experimental results.[18] On the other hand, h_3 is strongly hh-lh mixed with nodes in the wave function and small probability to optically recombine with s-like electrons. This explains why no evidence of h_3 is observed in the PL. The electron-electron (e-e), hole-hole (h-h), and electron-hole (e-h) direct Coulomb and long-range exchange-scattering matrix elements are computed from the single-particle states e_1, h_1, and h_2, and subsequently injected into a many-body configuration interaction (CI) Hamiltonian.[23] The small (10–30 %) contribution from short-range e-h exchange interactions is neglected.[24] For simplicity we also neglect scattering with (continuum) VQWR states. It was verified that the exclusion of h_3 from the CI does not affect the final results. The computed emission energy is 1544 meV for $X_{\bar{1}0}$ (1552 meV for $X_{0\bar{1}}$), close to the measured value 1545 ± 2.5 meV (1551 ± 2.4 meV), as averaged over the ensemble of the measured dots.

The computed PL spectrum of $X_{\bar{1}0}$ is shown in Fig. 3(c). Due to the $E_{3/2}$ symmetry of h_1, the spectrum lacks any vertically polarized components, despite that the hole character is not purely hh. Thus, the part of the dipole-matrix element related to the ~11% lh of h_1 character vanishes. Note that the spectrum is totally dominated by its high-energy component, indicating that the symmetry of $X_{\bar{1}0}$ is approximately

D_{3h} [Fig. 1(b) (left, thick lines)]. This is not surprising since the chosen dot shape exhibits D_{3h} symmetry and the C_{3v} contribution from the piezoelectric field is small. However, we will now demonstrate that the experimentally observed fine structure can essentially be understood in terms of an exciton of elevated symmetry D_{3h}, subjected to an anisotropic perturbation lowering the symmetry to C_{2v}. *This means, in particular, the presence of an additional approximate horizontal symmetry plane in all the quantum states involved.* The perturbation is introduced in the model by truncating one corner of the triangular QD cross section according to the inset of Figs. 3(d) and 3(e) ($b=12.5$ nm) and the corresponding spectra of $X_{\bar{1}0}$ and $X_{0\bar{1}}$ are shown in Figs. 3(d) and 3(e). It is clear that the perturbation introduces the predicted splitting of the in-plane polarized components for both $X_{\bar{1}0}$ and $X_{0\bar{1}}$. More remarkable is that the almost dark component of $X_{\bar{1}0}$ [Fig. 3(c)] becomes optically active with vertical polarization [Fig. 3(d)]. Thus, we interpret the weak vertically polarized component experimentally observed for $X_{\bar{1}0}$ [Fig. 3(a)] as the dark state of a D_{3h} exciton turned slightly bright by symmetry breaking.

The computed intensities and energy order of all exciton features in $X_{\bar{1}0}$ and $X_{0\bar{1}}$ match remarkably well with experiment [cf. Figs. 3(a), 3(b), 3(d), and 3(e)]. However, the computed splittings are smaller than the experimental ones; the computed splitting for $X_{\bar{1}0}$ ($X_{0\bar{1}}$) is 70 μeV (47 μeV) and the measured value is 185 ± 20 μeV (150 ± 15 μeV). Thus, the valence-conduction band mixing is not fully represented by the model, probably due to the limited number of states included in the CI.

Finally, we will discuss the hh-lh hybrid trion X_{11}^+, which, in addition to the e-h exchange interaction, also involves the h-h exchange interaction. We start with a group theoretical treatment of the symmetric cases (D_{3h} and C_{3v}), for which the h-h exchange energy between $h_1(E_{1/2})$ and $h_2(E_{3/2})$ splits the eight states of X_{11}^+ into two pairs of Kramers doublets (KDs), as shown in Fig. 4(a) (left). Each pair is further split by the e-h exchange interaction. Upon the optical decay of $X_{1\bar{1}}^+$, two KDs have vertical polarization vector and the other two are polarized in-plane. Thus, breaking of the D_{3h} or C_{3v} symmetry is evidenced, if more than two components of $X_{1\bar{1}}^+$ are resolved in either polarization.

The PL of $X_{1\bar{1}}^+$ shown in Fig. 4(c) reveals indeed three vertically polarized components as well as three in-plane polarized components, confirming the symmetry breaking whose exact origin is presently unknown. We tentatively attribute it to deviations from perfectly symmetrical pyramidal recess just before dot deposition or slight anisotropic thickness distribution of the dot layer itself.

The spectral features of the trion are further quantitatively understood by the numerical model. X_{11}^+ is shown in Fig. 4(a) (right) and the resulting spectra of $X_{1\bar{1}}^+$ are shown in Fig. 4(b). In this asymmetric case, the h-h exchange interaction alone splits the upper pair of KDs while the lower pair remains nearly degenerate (<2 μeV splitting). The nearly degenerate pair of KDs is further split by e-h exchange, in a fashion analogous to the symmetric case, where one KD is optically active with vertical polarization while the other one has in-
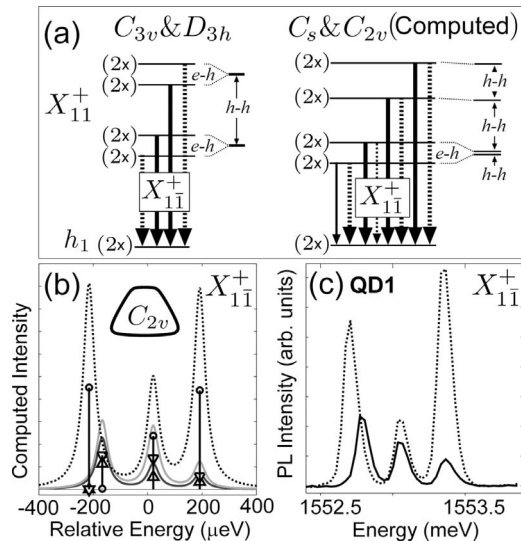
FIG. 4. (a) Polarized radiative decay paths of the positive trion X_{11} for the ideal case C_{3v} (left) and the asymmetric case C_s (right). The numerical model yield dark transitions indicated by thin lines and small arrows. Black solid lines indicate both x- and y-polarized light. Dotted lines indicate z-polarized light. (b) Computed exciton spectra of $X_{1\bar{1}}^-$ (see caption of Fig. 3). (c) Close-up PL of $X_{1\bar{1}}^+$.

plane polarization. In contrast, the two KDs split by the asymmetric part of the h-h exchange interaction are both optically active in all polarization directions. Since the asymmetric contribution of the h-h exchange splitting is essentially much larger than the corresponding e-h exchange, the excited states of $X_{1\bar{1}}^+$ is an efficient probe of a symmetry

breaking. Note that the lower pair of KDs of X_{11}^+ is virtually not affected by the asymmetry as reflected by its polarization properties, contributing only one line to $X_{1\bar{1}}^+$ instead of two in each of the polarizations [Figs. 4(b) and 4(c)].

Recently, the theoretical works of R. Singh *et al.*[25] and A. Schliwa *et al.*[26] on C_{3v} symmetric QDs have come to our attention. The assignment of a set of dark and bright transitions made in Ref. 25 is only consistent with an elevation of the symmetry to D_{3h}, as demonstrated by our symmetry analysis.

We emphasize that the concept of symmetry elevation, which we implemented to explain the radiative pattern of excitonic complexes, has a general validity going beyond the specific case of C_{3v} QDs. It is extremely useful in order to explain the origin of weaker and stronger radiative transitions from the same excitonic complex. This concept was initially discovered in a theoretical work of C_{3v} quantum wires.[27]

To conclude, the combination of group theory analysis and numerical $k \cdot p$ based CI calculations of the FSS of exciton complexes unveiled an additional approximate symmetry plane and small breaking of the high C_{3v} symmetry of pyramidal QDs. We predicted also that QDs with C_{3v} symmetry have degenerate bright states and are, thus, ideally suited as sources of polarization entangled photon pairs. Our analysis of the fine structure splitting based on symmetry has wide applicability because other types of QDs, Stranski-Krastanov or nanowire based, may also possess high symmetry when grown on (111) substrates and feature similar effects of symmetry breaking and symmetry elevation.

[1] O. Benson, C. Santori, M. Pelton, and Y. Yamamoto, Phys. Rev. Lett. **84**, 2513 (2000).

[2] G. Bester, S. Nair, and A. Zunger, Phys. Rev. B **67**, 161306(R) (2003).

[3] R. J. Young, R. M. Stevenson, P. Atkinson, K. Cooper, D. A. Ritchie, and A. J. Shields, New J. Phys. **8**, 29 (2006).

[4] R. Hafenbrak, S. M. Ulrich, P. Michler, L. Wang, A. Rastelli, and O. G. Schmidt, New J. Phys. **9**, 315 (2007).

[5] N. Akopian, N. H. Lindner, E. Poem, Y. Berlatzky, J. Avron, D. Gershoni, B. D. Gerardot, and P. M. Petroff, Phys. Rev. Lett. **96**, 130501 (2006).

[6] R. M. Stevenson, R. J. Young, P. Atkinson, K. Cooper, D. A. Ritchie, and A. J. Shiel, Nature (London) **439**, 179 (2006).

[7] L. He, M. Gong, C. F. Li, G. C. Guo, and A. Zunger, Phys. Rev. Lett. **101**, 157405 (2008).

[8] T. Warming, E. Siebert, A. Schliwa, E. Stock, R. Zimmermann, and D. Bimberg, Phys. Rev. B **79**, 125316 (2009).

[9] B. Urbaszek, R. J. Warburton, K. Karrai, B. D. Gerardot, P. M. Petroff, and J. M. Garcia, Phys. Rev. Lett. **90**, 247403 (2003).

[10] M. E. Ware, E. A. Stinaff, D. Gammon, M. F. Doty, A. S. Bracker, D. Gershoni, V. L. Korenev, S. C. Bădescu, Y. Lyanda-Geller, and T. L. Reinecke, Phys. Rev. Lett. **95**, 177403 (2005).

[11] M. Bayer *et al.*, Phys. Rev. B **65**, 195315 (2002).

[12] S. L. Altmann and P. Herzig, *Point-Goup Theory Tables* (Clarendon Press, Oxford, 1994).

[13] D. Y. Oberli, M. Byszewski, B. Chalupar, E. Pelucchi, A. Rudra, and E. Kapon, Phys. Rev. B **80**, 165312 (2009).

[14] M. H. Baier, S. Watanabe, E. Pelucchi, and E. Kapon, Appl. Phys. Lett. **84**, 1943 (2004).

[15] G. Biasiol, A. Gustafsson, K. Leifer, and E. Kapon, Phys. Rev. B **65**, 205306 (2002).

[16] Q. Zhu, E. Pelucchi, S. Dalessi, K. Leifer, M.-A. Dupertuis, and E. Kapon, Nano Lett. **6**, 1036 (2006).

[17] A. Hartmann, Y. Ducommun, K. Leifer, and E. Kapon, J. Phys.: Condens. Matter **11**, 5901 (1999).

[18] K. F. Karlsson, V. Troncale, D. Y. Oberli, A. Malko, E. Pelucchi, A. Rudra, and E. Kapon, Appl. Phys. Lett. **89**, 251113 (2006).

[19] M. H. Baier, A. Malko, E. Pelucchi, D. Y. Oberli, and E. Kapon, Phys. Rev. B **73**, 205321 (2006).

[20] V. Troncale, K. F. Karlsson, D. Y. Oberli, M. Byszewski, A. Malko, E. Pelucchi, A. Rudra, and E. Kapon, J. Appl. Phys. **101**, 081703 (2007).

[21] See supplementary material at http://link.aps.org/supplemental/10.1103/PhysRevB.81.161307 for additional information.

[22] I. Vurgaftman, J. R. Meyer, and L. R. Ram-Mohan, J. Appl. Phys. **89**, 5815 (2001).

[23] A. Barenco and M. A. Dupertuis, Phys. Rev. B **52**, 2766 (1995).

[24] J. Luo, G. Bester, and A. Zunger, New J. Phys. **11**, 123024 (2009).

[25] R. Singh and G. Bester, Phys. Rev. Lett. **103**, 063601 (2009).

[26] A. Schliwa, M. Winkelnkemper, A. Lochmann, E. Stock, and D. Bimberg, Phys. Rev. B **80**, 161307(R) (2009).

[27] S. Dalessi, F. Michelini, and M. A. Dupertuis (unpublished).